

Constraining possible variations of the fine structure constant in strong gravitational fields with the $K\alpha$ iron line

Cosimo Bambi

Center for Field Theory and Particle Physics & Department of Physics,
Fudan University, 220 Handan Road, 200433 Shanghai, China

E-mail: bambi@fudan.edu.cn

Abstract. In extensions of general relativity and in theories aiming at unifying gravity with the forces of the Standard Model, the value of the “fundamental constants” is often determined by the vacuum expectation value of new fields, which may thus change in different backgrounds. Variations of fundamental constants with respect to the values measured today in laboratories on Earth are expected to be more evident on cosmological timescales and/or in strong gravitational fields. In this paper, I show that the analysis of the $K\alpha$ iron line observed in the X-ray spectrum of black holes can potentially be used to probe the fine structure constant α in gravitational potentials relative to Earth of $\Delta\phi \approx 0.1$. At present, systematic effects not fully under control prevent to get robust and stringent bounds on possible variations of the value of α with this technique, but the fact that current data can be fitted with models based on standard physics already rules out variations of the fine structure constant larger than some percent.

Keywords: astrophysical black holes, gravity, X-rays

Contents

1	Introduction	1
2	$K\alpha$ iron line	2
3	Constraints	3
4	Discussion	6
5	Summary and conclusions	8
A	Theories violating the Einstein Equivalence Principle	8
B	Photon propagation in the background metric	10
C	Error analysis	10

1 Introduction

The Einstein Equivalence Principle (EEP) is a fundamental concept in general relativity and in other theories of gravity. It is based on the following three assumptions [1]:

1. Weak Equivalence Principle (WEP). The trajectory of a freely-falling test-particle is independent of its internal structure and composition.
2. Local Lorentz Invariance (LLI). The result of any local non-gravitational experiment is independent of the velocity of the freely-falling reference frame in which it is performed.
3. Local Position Invariance (LPI). The result of any local non-gravitational experiment is independent of where and when in the Universe it is performed.

The WEP is equivalent to the statement that the “inertial mass” is always proportional to the “gravitational mass”, and therefore we can choose a system of units in which such a proportionality constant is 1. Moreover, it seems (Schiff’s conjecture) that any complete and self-consistent theory of gravity in which the WEP holds necessarily implies the LLI and the LPI, and therefore the EEP [1]. However, a rigorous proof on such a conclusion is lacking. The EEP is satisfied by metric theories of gravity, including general relativity and all those frameworks in which the spacetime is characterized by a symmetric metric and possible new degrees of freedom universally couple to matter.

Extensions of general relativity and theories aiming at unifying gravity with the forces of the Standard Model typically violate the EEP [2–10] (see also Appendix A). Tests of the EEP can thus be seen as an alternative strategy to discover new interactions and they can potentially find signatures of high energy physics in the low energy gravity sector. The search for time and/or space variations of fundamental constants is a quite hot topic today and can involve different research fields [11, 12]. It is a test of the LPI, and therefore of the EEP. For instance, in superstring theories, the low energy parameters of the Standard Model depend on the vacuum expectation value of scalar fields (dilaton, moduli). As the latter is

determined by the background geometry, it is quite natural to expect both temporal variation on cosmological scales and a dependence on the gravitational potential of the values of these quantities. However, clear predictions are not possible, and the common strategy is to adopt a phenomenological approach, constraining possible variations of fundamental constants in many different ways.

The possibility of time and/or space variations of the fine structure constant $\alpha = e^2/\hbar c \approx 1/137$ has attracted a lot of interest. Atomic clock experiments can constrain possible temporal variations of α today at the level of $|\dot{\alpha}/\alpha| \lesssim 10^{-17} \text{ yr}^{-1}$ [13]. In Ref. [14, 15], the authors reported evidence for a different value of α in quasar spectra at high redshift, which was initially interpreted as an indication for a temporal variation of the fine structure constant. More recent studies seem instead to point out a spacial variation of α , with the existence of a preferred direction in the Universe: for redshift $z > 1.8$, data from the Keck telescope for the Northern sky suggest $\Delta\alpha/\alpha = (-0.74 \pm 0.17) \cdot 10^{-5}$, while data from the VLT telescope for the Southern sky give $\Delta\alpha/\alpha = (+0.61 \pm 0.20) \cdot 10^{-5}$ [16]. While it is not clear how robust these results are, they cannot be explained by the known systematic effects. The dependence of the fine structure constant on strong gravitational fields has been studied in [17]. The authors compare laboratory spectra with far-UV astronomical spectra from the white-dwarf star G191-B2B and obtain the constraints

$$\begin{aligned} \Delta\alpha/\alpha &= (4.2 \pm 1.6) \cdot 10^{-5} \quad (\text{FeV}), \\ \Delta\alpha/\alpha &= (-6.1 \pm 5.8) \cdot 10^{-5} \quad (\text{NiV}), \end{aligned} \tag{1.1}$$

for a dimensionless gravitational potential relative to Earth of $\Delta\phi \approx 5 \cdot 10^{-5}$, where $\phi = G_N M/r c^2$, M is the mass of the white dwarf/Earth, and r its radius.

2 $K\alpha$ iron line

The X-ray spectrum of black hole candidates is often characterized by the presence of a power-law component. This feature is commonly interpreted as the inverse Compton scattering of thermal photons by electrons in a hot corona above the accretion disk. This “primary component” irradiates also the accretion disk, producing a “reflection component” and spectral lines by fluorescence in the X-ray spectrum. The strongest line is the $K\alpha$ iron line at 6.4 keV. This line is intrinsically narrow in frequency, while the one observed appears broadened and skewed. The interpretation is that the line is strongly altered by special and general relativistic effects, which produce a characteristic profile, first predicted and identified from Cygnus X-1 data in Ref. [18] (though that observation was originally published in [19]). For a review, see e.g. Refs. [20, 21].

The profile of the $K\alpha$ iron line depends on the background metric, the geometry of the emitting region, the disk emissivity, and the disks inclination angle with respect to the line of sight of the distant observer. In 4-dimensional general relativity, black holes are described by the Kerr solution and are characterized by only two parameters; that is, the mass M and the spin angular momentum J . The dimensionless spin parameter $a_* = J/M^2$ is the only relevant parameter of the background geometry, while M sets the length of the system, without affecting the line profile. In those sources for which there is indication that the line is mainly emitted close to the compact object, the emission region is thought to range from the radius of the innermost stable circular orbit (ISCO), $r_{\text{in}} = r_{\text{ISCO}}$, to some outer radius r_{out} . The disk emissivity is often assumed to be a power-law in radius of the form $I_e \propto 1/r^q$. The simple lamp-post model gives $q = 3$ at large radii $r \gg r_g$, where $r_g = G_N M/c^2$ is the

gravitational radius of the object. This becomes a quite bad approximation for the inner accretion disk, which can be very important for the spin measurement of fast-rotating black holes. In Ref. [22], the authors compute the emissivity index q in the lamp-post model as a function of the radial coordinate for different lamp-post heights (see their Fig. 3). In practice, one often assumes an inner and an outer emissivity indices, say q_1 and q_2 , which are determined during the fitting procedure [23]. The fourth parameter is the inclination of the disk with respect to the line of sight of the distant observer, i . The dependence of the line profile on a_* , i , q , and r_{out} in the Kerr background has been analyzed in detail by many authors, starting from Ref. [18]. The profile of the $K\alpha$ iron line in non-Kerr spacetimes is discussed in Refs. [24–28].

The spin parameter a_* determines the ISCO radius, ranging from r_g for $a_* = 1$ (maximally rotating black hole and corotating accretion disk) to $6r_g$ for $a_* = 0$ (non-rotating black hole), and $9r_g$ for $a_* = -1$ (maximally rotating black hole and counterrotating accretion disk). As shown in the left panel of Fig. 1, a_* can be inferred from the low energy tail of the line, which is produced by the strong gravitational redshift at small radii. The right panel of Fig. 1 shows instead the effect of the inclination angle i on the line profile: a higher (lower) inclination angle moves the high energy cut-off to higher (lower) energies, with small effects on the extension of the low energy tail¹. Indeed, the cut-off is produced by Doppler blueshift at relatively large radii, approximately in the region $7 < r/r_g < 25$ (left panel of Fig. 2). Doppler boosting is maximum for edge-on disks ($i \rightarrow 90^\circ$) and vanishes for face-on disks ($i \rightarrow 0^\circ$).

3 Constraints

The position of the high energy cut-off, which is determined by i in the standard theory, may also be changed by a variation of the energy of the line. This is shown in the right panel of Fig. 2. The energy of the $K\alpha$ iron line is set by the Rydberg energy,

$$E_{K\alpha} \sim \frac{\alpha^2 m_e c^2}{2} (Z - 1)^2, \quad (3.1)$$

where m_e is the electron mass and $Z = 26$ the atomic number of the iron. If we can have an independent measurement of the inclination angle of the accretion disk, the determination of the position of the high energy cut-off of the $K\alpha$ iron line can potentially measure the value of $\alpha^2 m_e$ in a gravitational potential relative to Earth of $\Delta\phi \approx 0.1$ (or the value of α , if we assume that the electron mass cannot change). Let us note that here photons are emitted from the accretion disk, propagate in a Kerr spacetime, and eventually reach the X-ray detector, which measures the photon energy with the value of the fundamental constants on Earth. So, we are effectively comparing the energy of the $K\alpha$ iron line in the region around the black hole with the one measured on Earth. We can potentially constrain the value of fundamental constants with a single energy line because we can calculate the redshift factor. In Refs. [14–17], the authors have to consider two lines with different α -dependence because

¹In Fig. 1, the photon flux is normalized as $\int_0^\infty N(E)dE = 1$ (see Ref. [25]) and this causes a certain dependence of the low energy photon flux on i . While the inclination angle surely alters the Doppler redshift/blueshift, the effect is subdominant with respect to the gravitational redshift and therefore the low energy tail is mainly determined by the black hole spin parameter. If we focus on the low energy tail, we can use the normalization $\int_0^{3.5 \text{ keV}} N(E)dE = 1$. For a black hole with $a_* = 0.98$, the photon flux at 3.5 keV varies less than 8% changing i in the range $0^\circ - 65^\circ$, and something more in the range $0^\circ - 90^\circ$.

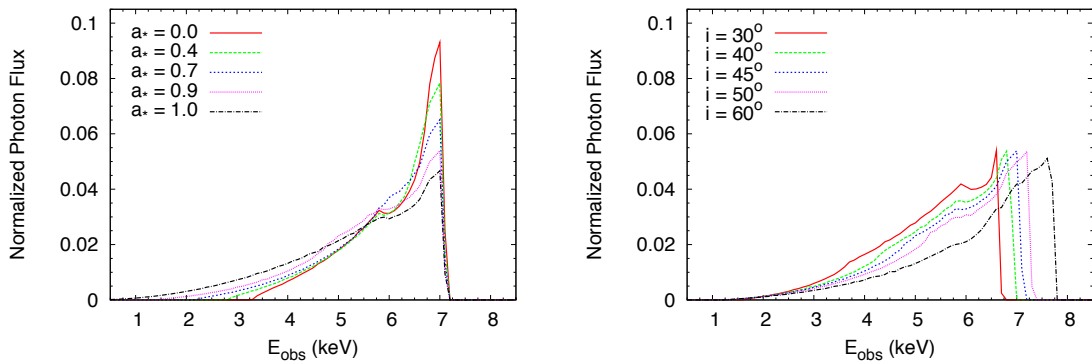


Figure 1. Left panel: $K\alpha$ iron line in Kerr spacetime with different values of the spin parameter a_* and viewing angle $i = 45^\circ$. Right panel: $K\alpha$ iron line in Kerr spacetime with spin parameter $a_* = 0.9$ and different values of the viewing angle i . The other parameters of the model are: inner radius $r_{\text{in}} = r_{\text{ISCO}}$, outer radius $r_{\text{out}} = r_{\text{in}} + 100 r_g$, index of the emissivity profile $q = 3$.

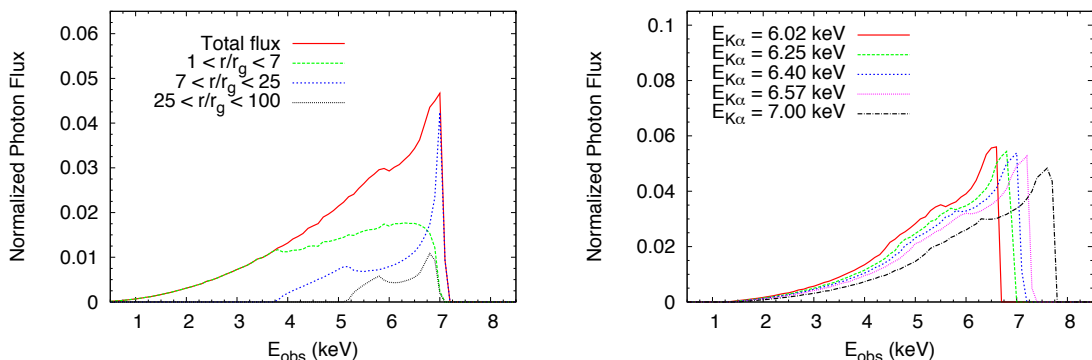


Figure 2. Left panel: $K\alpha$ iron line in Kerr spacetime with spin parameter $a_* = 1$, viewing angle $i = 45^\circ$, inner radius $r_{\text{in}} = r_{\text{ISCO}} = r_g$, outer radius $r_{\text{out}} = 100 r_g$, index of the emissivity profile $q = 3$; the panel shows the total flux as well as the corresponding contributions from the disk regions $1 < r/r_g < 7$, $7 < r/r_g < 25$, and $25 < r/r_g < 100$. The high energy cut-off in the spectrum is due to Doppler blueshift at radii $7 < r/r_g < 25$. Right panel: As in the right panel of Fig. 1, with viewing angle $i = 45^\circ$ and different values of $E_{K\alpha}$.

the redshift factor is not known and therefore with a single line one can only measure a combination of the redshift and of the value of α .

Independent estimates of the inclination of the disk are possible. Detection of EEP violation relies on an “apparent” misalignment between the inclination angle of the inner disk (inferred from the iron line) and the angle of the orbital plane of the binary system (obtained from optical/near-infrared light curve measurements) or the angle of the jet. The crucial assumption of this approach is therefore that there is no “real” misalignment between the inclination of the inner disk and the reference one. If the jet is powered by the black hole spin, strictly speaking the jet measurement provides the inclination angle of the spin. However, the Bardeen-Petterson effect should quickly align the inner accretion disk to the

Source	i (deg)	Iron				$\Delta\alpha/\alpha$
		i range (deg)	i (deg)	a_*	Ref.	
Cygnus X-1	27.1 ± 0.8 (O) [32]	free	30 ± 1	0.05 ± 0.01	[36]	0.005 ± 0.003
		free	32 ± 2	$0.88^{+0.07}_{-0.11}$	[37]	0.008 ± 0.005
		free	$23.7^{+6.7}_{-5.4}$	$0.97^{+0.014}_{-0.02}$	[23]	$-0.005^{+0.011}_{-0.007}$
		free	$39.8^{+3.0}_{-4.2}$	> 0.98	[23]	$0.023^{+0.008}_{-0.010}$
		free	> 40	> 0.83	[38]	> 0.023
GRS 1915+105	66 ± 2 (J) [33]	$65 \leq i \leq 80$	72 ± 1	0.98 ± 0.01	[39]	0.027 ± 0.014
GRO J1655-40	70.2 ± 1.2 (O) [34]	$69 \leq i \leq 85$	69^{+1}	0.98 ± 0.01	[36]	$-0.006^{+0.010}$
4U 1543-475	20.7 ± 1.5 (O) [34]	$20 \leq i \leq 22$	22_{-1}	0.3 ± 0.1	[36]	$0.0016_{-0.0031}$
XTE J1550-564	74.7 ± 3.8 (O) [35]	$50 \leq i \leq 80$	50^{+1}	0.76 ± 0.01	[36]	$-0.023^{+0.004}$
		$60 \leq i \leq 82$	82_{-3}	$0.55^{+0.15}_{-0.22}$	[40]	$0.003_{-0.003}$
	71^{+12}_{-7} (J) [31]					

Table 1. List of the stellar-mass black hole candidates for which the inclination angle i can be inferred from the analysis of the $K\alpha$ iron line and from at least another method. Strictly speaking, optical/near-infrared observations (O) determine the inclination angle of the orbital plane of the binary system. The measurements of the inclination angle of the jet (J) should at least reflect the orientation of the black hole spin. See the text for details.

black hole spin [29]. If the jet is powered by the rotational energy of the disk, its measurement automatically gives the inclination angle of the inner disk. The orbital plane of the binary system is obtained from optical/near-infrared observations of the stellar companion and of the accretion disk at large scales. In the case of an initial misalignment with the black hole spin, the disk forces the black hole to alignment with a time scale of order $10^6 - 10^8$ yrs [30, 31]. Such a time is typically shorter than the age of the system, so that (in the worst situation, i.e. measurement of the inclination angle of the orbital plane and initial misalignment with the black hole spin) one could expect that only 1 – 2% of the black hole binary systems with an initial misalignment are still misaligned. Let us notice that the original alignment timescale estimated in Ref. [30] was overestimated by a factor 50 due to a numerical error in Eq. (6) of that paper.

Tab. 1 shows the list of black holes in X-ray binary systems for which an estimate of the inclination angle from both dynamical/jet methods and analysis of the iron line are reported in the literature [23, 32–40]. The first column reports the name of the source and the second column the estimate of i from optical/near-infrared light curve (O) and jet (J) measurements. The third, fourth, fifth, and sixth columns are for the measurements obtained from the analysis of the $K\alpha$ iron line. As the shape of the line depends on several free parameters, the fitting procedure is very time consuming, while the data are not always very good. It is thus common to restrict the range of the free parameters on the basis of independent estimates. The fourth column shows exactly the range of i adopted in these studies. Cygnus X-1 has been studied in Refs. [23, 36–38], always leaving i completely free. The low spin parameter found in Ref. [36] seems to be due to both improper data state (the source was not in the high/soft state) and the improper usage in the continuum model in extracting the skewed iron line profile (see discussion in Section 7.1 of [41]). The two inclination angles found in Ref. [23] refer to two different models: the lower value is provided by a model with two emissivity indices obtained from the fit, while the higher one by a model

with $q = 3$. The authors of Ref. [38] consider several models, and the ones that provide good fits have inclination angles ranging between 40° and 69° . Such a model-dependent inclination angle in the results of Ref. [38] may come from missing physics, which was not important in observations of satellites like Chandra and XMM-Newton, but that cannot be ignored for NuSTAR. The seventh column of Tab. 1 shows the measurements of the variation of the fine structure constant α (assuming that m_e is a true constant) obtained by comparing a line at $E = 6.40$ keV with i given by the fifth column with lines resulting from a variable rest-frame energy and an inclination angle given by the first column of Tab. 1. Since the aim of the present paper is just to propose this technique to constrain possible variation of the fine structure constant in strong gravitational field, the bounds on $\Delta\alpha/\alpha$ reported in Tab. 1 have been obtained by comparing two theoretical models, not from actual data, which simplifies the analysis a lot. The other model parameters are fixed, because the high energy cut-off of the iron line profile is not very sensitive to them (see Appendix C for the details). The procedure to determine $\Delta\alpha/\alpha$ is described in Appendix C.

4 Discussion

Based on the simplified approach discussed in Appendix C that does not analyze real data but compares two theoretical models with the measurements reported in the literature, one can find the constraints on possible variations of the fine structure constant α in the gravitational fields of stellar-mass black holes shown in the last column of Tab. 1. The uncertainties on $\Delta\alpha/\alpha$ are smaller than the differences between the bounds inferred from different measurements and sources, which suggests that there are systematics effects not properly taken into account. However, if we consider the spread of these constraints as uncertainty, we can argue that the X-ray data are consistent with no variations of α larger than some percent. If we exclude the measurements reported in Ref. [38], all the constraints converge to $|\Delta\alpha/\alpha| < 3\%$. In Ref. [38], the authors consider different models and the ones with a good fit require an inclination angle in the range 40° and 69° . If the dynamical estimate of i from Ref. [32] is correct and there is not a misalignment between the inner accretion disk and the orbital plane of the binary system, these measurements would suggest a non-vanishing $\Delta\alpha/\alpha$ in the range 2 – 10%. However, a $\Delta\alpha/\alpha$ exceeding 3% would disagree with all the other results reported in the literature and can be probably excluded.

All the bounds have to be taken with some caution. In the case of the measurements reported in Ref. [23] for the inclination angle of the inner disk of Cygnus X-1, the author find $i = 23.7^\circ$ consistent with the dynamical method for a model with two emissivity indices, q_1 and q_2 , both assumed as free parameters and determined in the fitting procedure. The angle $i = 39.8^\circ$ is instead found for a model with $q = 3$. While the first model should be more reliable, this example shows the impact on the choice of the exact/wrong model to constrain variations of the fine structure constant.

In the case of the black hole binaries in 4U 1543-475, GRO J1655-40, and XTE J1550-564, the inclination angle is not really a free parameter, but it is allowed to vary in a small range. For 4U 1543-475 studied in [36], the range is so small that i is effectively constrained by the optical observations, and therefore the bound on α is useless. For GRO J1655-40 and XTE J1550-564, the initial range of i is larger, but the fits require values at the boundary of the allowed range, so meaningful constraints can be put only on one side. For XTE J1550-564, the two measurements of the iron line are not consistent each other, and there exists also

an estimate of the inclination angle of the jet whose uncertainty exceeds the allowed range of i in the analysis of Refs. [31, 36] (and for this reason it has not been used in Tab. 1).

As already pointed out, the bounds reported in Tab. 1 have been obtained from a simple analysis without using actual X-ray data, just to show how this approach can work and get a crude estimate of possible constraints. In the case of real data, the situation is more complicated. For the highly ionized gas in X-ray binaries, atoms are in different ionization states and therefore the spectrum is a combination of several lines, ranging from 6.6 to 7.0 keV [20, 21]. The exact spectrum depends on the “ionization parameter”, which changes the relative contribution of the different ionization states. Different groups have computed tables of reflection spectra via radiative transfer for an illuminated atmosphere for a range of metallicities, densities, spectral indices, incident fluxes, and ionization parameters. In the studies reported in Tab. 1, the authors use these tables, not the value 6.4 keV. The fact that there is a spectrum rather than a single line makes the analysis more complicated, but it should not alter the ability to constrain $\Delta\alpha/\alpha$ if all the astrophysical details are properly taken into account. The ionization parameter is inferred by the fit, but the key-point is that the correlation between the ionization parameter and the inclination angle is not large [42]. If the ionization parameter is determined correctly, the exact spectrum is known. Let us also note that even the cleanest neutral 6.4 keV line is never a single line, but a blend of two lines that differ in energy by about 0.3%. That is further complicated by the fact that multiple ionization states each with multiple iron ion species radiate in different regions of the disk. The determination of the exact spectrum is currently the main source of uncertainty for the estimate of the viewing angle which, otherwise, could be determined with higher precision. While it is beyond the scope of the present paper to properly address this problem, it is definitively a key-issue in the future use of the $K\alpha$ iron line to test the value of the fine structure constant in the strong gravitational field of black holes. Intuitively, it seems that this is just a complication, but that it does not affect the method once the exact spectrum is determined, because it should just manifest as a shift which cancels out in the fit. However, the issue requires a much more detailed investigation, to exclude a possible correlation between the value of α and the estimate of the spectrum, which otherwise would invalidate or at least weaken this method to constrain α from the iron line profile.

In the study reported in this paper, the Kerr solution has been assumed as background metric. Actually, black holes in alternative theories of gravity may be described by other solutions. In those theories in which modifications to general relativity are Planck scale suppressed in the infrared, the Kerr metric is a good approximation. In the other cases, the position of the high energy cut-off of the iron line may be slightly different from the one around a Kerr black hole with the same viewing angle. That is mainly the result of a different orbital velocity of the gas. The angle i inferred from the iron line assuming (erroneously) the Kerr metric can be the correct one or be different by 1-2 degrees with respect to the true angle (sometimes even more), depending on the specific background [25, 26, 28]. An observation confirming the same value of α as the one on Earth could suggest that this is not the case, but in principle one cannot really exclude a fine compensation between a non-vanishing variation of α and a different Doppler blueshift producing an effect of the same magnitude but of opposite sign. Such a possibility can be ruled out in the case of measurements of i from sources with different inclination angle.

Since the value of fundamental constants like α may be determined by the vacuum expectation value of some fields, the analysis of the $K\alpha$ iron line can test the existence of hairy black holes [43–47]. The presence of fields non-universally coupled to matter would

affect also the motion of particles. In other words, we should expect also a violation of the WEP. However, one can see that such a possibility does not affect the calculations of the $K\alpha$ iron line. As shown in Appendix B, photons still follow the null geodesics of the spacetime, and therefore the calculation of the photon trajectories from the disk to the plane image of the distant observer is unaltered. Modifications of the photon trajectories would require additional new physics, like a term in the Lagrangian that provides mass to the photons. The properties of the trajectories of the gas’s particles in the disk are also not affected by possible variations of α , because they follow circular orbits, and therefore they feel the same value of α as a consequence of the axisymmetric background.

5 Summary and conclusions

Time and/or space variations of fundamental constants violate the EEP. The validity of the EEP is a fundamental ingredient in general relativity, but its violation is often expected in alternative theories of gravity and in theories aiming at unifying gravity with the forces of the Standard Model. Today there is no clear evidence of variations of fundamental constants, but observations of quasar spectra at high redshift hint at different values of the fine structure constant $\alpha = e^2/\hbar c$ with respect to the one measured on Earth [14–16]. A possible dependence of α on gravitational fields has been recently constrained in Ref. [17] from the far-UV spectra of a white-dwarf star, thus probing a gravitational potential relative to Earth of $\Delta\phi \approx 5 \cdot 10^{-5}$, and the bound is $|\Delta\alpha/\alpha| \lesssim 10^{-4}$. In this work, I showed that the position of the high energy cut-off in the profile of broad $K\alpha$ iron lines observed in the X-ray spectrum of black holes can be used to test α in much stronger gravitational fields, where $\Delta\phi \approx 0.1$, when an independent measurement of the disk’s inclination angle is available. At present, there are systematic effects not fully under control, and therefore this technique cannot provide robust and stringent constraints on α . Based on a simplified approach that does not analyze real data but compares two theoretical models with the measurements reported in the literature, I obtained the bounds in the last column of Tab. 1. The uncertainty on these constraints is smaller than their difference, which suggests that at least in some studies the systematics has not been properly taken into account. However, all the measurements are consistent with no variation of α large than some percent. This can be considered the present crude bound on possible variations of α with this approach. Even if we consider the measurements reported in Ref. [38], in which the authors find an inclination angle exceeding 40° and up to 69° , the data could still be explained with a variation of α lower than 2 – 10% (but a $\Delta\alpha/\alpha > 3\%$ seems unlikely because in disagreement with all the other studies). If in the future it is possible to have all the systematics under control, constraints of $\Delta\alpha/\alpha$ better than 1% with this technique do not seem to be out of reach.

A Theories violating the Einstein Equivalence Principle

The theories satisfying the EEP are called “metric theories of gravity” as they meet the following assumptions (for more details, see Ref. [1]):

1. The spacetime is endowed with a symmetric metric.
2. The trajectories of freely-falling test-particles are the geodesics of that metric.
3. In any local freely-falling reference frame, the non-gravitational laws of physics reduce to the ones of special relativity.

General relativity is clearly a metric theory of gravity. Tensor-scalar theories are metric theories of gravity if the additional degrees of freedom universally couple to matter. For instance, if we consider a theory in which the gravity sector is described by the spacetime metric $g_{\mu\nu}$ and by a scalar field ϕ , and gravity is universally coupled to matter, the total action looks like

$$S = S_g[g_{\mu\nu}, \phi] + S_m[\psi_{m1}, \psi_{m2}, \dots, A^2(\phi)g_{\mu\nu}]. \quad (\text{A.1})$$

The crucial point that determines the fact that the action in (A.1) belongs to a metric theory of gravity is that the matter sector responds to the metric

$$\tilde{g}_{\mu\nu} = A^2(\phi)g_{\mu\nu}, \quad (\text{A.2})$$

and therefore we can perform the conformal transformation above and find that all the particles follow the geodesics of the metric $\tilde{g}_{\mu\nu}$ and that the result of any local non-gravitational experiment must meet both the LLI and the LPI. On the other hand, if the new degrees of freedom do not universally couple to matter, such a transformation is not possible. If the total action is

$$S = S_g[g_{\mu\nu}, \phi] + S_{m1}[\psi_{m1}, A^2(\phi)g_{\mu\nu}] + S_{m2}[\psi_{m2}, B^2(\phi)g_{\mu\nu}], \quad (\text{A.3})$$

we can still perform the conformal transformation in Eq. (A.2), but now we find that the particles associated to the field ψ_{m1} follow the geodesics of the metric $\tilde{g}_{\mu\nu}$, but the ones associated to the field ψ_{m2} do not; that is, the WEP is violated. The transformation

$$\hat{g}_{\mu\nu} = B^2(\phi)g_{\mu\nu} \quad (\text{A.4})$$

does not fix the problem: now the particles associated to ψ_{m2} follow the geodesics of the metric $\hat{g}_{\mu\nu}$, but the ones associated to ψ_{m1} do not. The EEP turns out to be violated in many extensions of general relativity.

Let us now assume that all the elementary particles responds to the metric $g_{\mu\nu}$. The electromagnetic action can be [8–10]

$$S_{\text{em}} = \frac{1}{4g_{\text{em}}^2} \int \sqrt{-g} C^2(\phi) g^{\mu\nu} g^{\rho\sigma} F_{\mu\rho} F_{\nu\sigma} d^4x, \quad (\text{A.5})$$

where g_{em} is the “actual” electromagnetic coupling and $F_{\mu\nu}$ is the strength of the electromagnetic field. The “effective” electromagnetic constant turns out to be

$$\alpha = g_{\text{em}}^2 C^{-2}(\phi), \quad (\text{A.6})$$

and, if ϕ is not constant, the LPI can be violated. From the new Maxwell’s equations, one can see that photons still follow the null geodesics of the metric $g_{\mu\nu}$ (see Appendix B). In general, a space and/or time variations of the fine structure constant implies also a violation of the WEP, because the mass of particles like protons and neutrons receives contributions from the electromagnetic interaction and therefore spacetime variations of α necessarily imply spacetime variations of their masses, which violates the equivalence between inertial and gravitational mass. However, the calculations of the profile of the $K\alpha$ iron line only involve the properties of equatorial circular orbits of the gas’s particles, which are not affected by a possible dependence of α on ϕ for axisymmetric backgrounds.

B Photon propagation in the background metric

In the standard theory, Maxwell's equations $\nabla_\nu F^{\mu\nu} = 0$ imply that photons follow the null geodesics of the background metric, see e.g. Section 22.5 of Ref. [48]. Indeed, from the identity

$$\nabla_\nu \nabla^\mu A^\nu = \nabla^\mu \nabla_\nu A^\nu + R^\mu{}_\nu A^\nu \quad (\text{B.1})$$

and the Lorentz gauge condition $\nabla_\nu A^\nu = 0$, Maxwell's equations $\nabla_\nu F^{\mu\nu} = 0$ become

$$R^\mu{}_\nu A^\nu - \nabla_\nu \nabla^\nu A^\mu = 0. \quad (\text{B.2})$$

In the geometrical optics approximation, the electromagnetic potential A_μ can be written as

$$A_\mu = \text{Re} \left[(a_\mu + \epsilon b_\mu + \epsilon^2 c_\mu + \dots) e^{i\Theta/\epsilon} \right], \quad (\text{B.3})$$

where $\epsilon \ll 1$ is an expansion parameter. Light rays are defined as the curves normal to the surfaces of constant phase Θ . The wave vector k^μ is given by $k^\mu = \nabla^\mu \Theta$. If we plug Eq. (B.3) into Eq. (B.2), we have

$$\begin{aligned} \text{Re} \left\{ \left[\frac{1}{\epsilon^2} k_\nu k^\nu (a^\mu + \epsilon b^\mu + \epsilon^2 c^\mu + \dots) + \right. \right. \\ \left. \left. - \frac{2i}{\epsilon} k^\nu \nabla_\nu (a^\mu + \epsilon b^\mu + \epsilon^2 c^\mu + \dots) - \frac{2i}{\epsilon} (\nabla_\nu k^\nu) (a^\mu + \epsilon b^\mu + \epsilon^2 c^\mu + \dots) + \right. \right. \\ \left. \left. + \nabla_\nu \nabla^\nu (a^\mu + \epsilon b^\mu + \epsilon^2 c^\mu + \dots) + R^\mu{}_\nu (a^\nu + \epsilon b^\nu + \epsilon^2 c^\nu + \dots) \right] e^{i\Theta/\epsilon} \right\} = 0. \quad (\text{B.4}) \end{aligned}$$

The leading order in the ϵ -expansion is $O(\epsilon^{-2})$ and gives $k_\nu k^\nu a^\mu = 0$, i.e. k^ν is a null vector. Since $\nabla_\nu k_\mu = \nabla_\mu k_\nu$, we have

$$\nabla_\mu (k_\nu k^\nu) = 0 \quad \Rightarrow \quad k^\nu \nabla_\mu k_\nu = 0, \quad (\text{B.5})$$

which implies that photon trajectories are the null geodesics of the metric $g_{\mu\nu}$.

If the action of the electromagnetic sector is the one in Eq. (A.5), the variation of the electromagnetic potential A_μ provides modified Maxwell's equations

$$\nabla_\nu [C^2(\phi) F^{\mu\nu}] = 0. \quad (\text{B.6})$$

If we use Eq. (B.3), we have

$$R^\mu{}_\nu A^\nu - \nabla_\nu \nabla^\nu A^\mu + \frac{2}{C} (\partial_\nu C) (\nabla^\mu A^\nu - \nabla^\nu A^\mu) = 0. \quad (\text{B.7})$$

Since $\nabla^\mu A^\nu - \nabla^\nu A^\mu = O(\epsilon^{-1})$, the leading order term of Maxwell's equations remains $k_\nu k^\nu a^\mu = 0$ and photons still follow the null geodesics of the background metric.

C Error analysis

Figs. 3-6 show the effect of the model parameters (spin a_* , viewing angle i , outer radius r_{out} , index of emissivity profile q) on the high energy cut-off of the iron line profile. Uncertainties like $\Delta a_* \sim 0.05 - 0.10$, $\Delta i \sim 1^\circ - 2^\circ$, and $\Delta q \sim 0.1 - 0.2$ are typical values found in the iron line analysis. *The plots show that the effect of the viewing angle is qualitatively different*

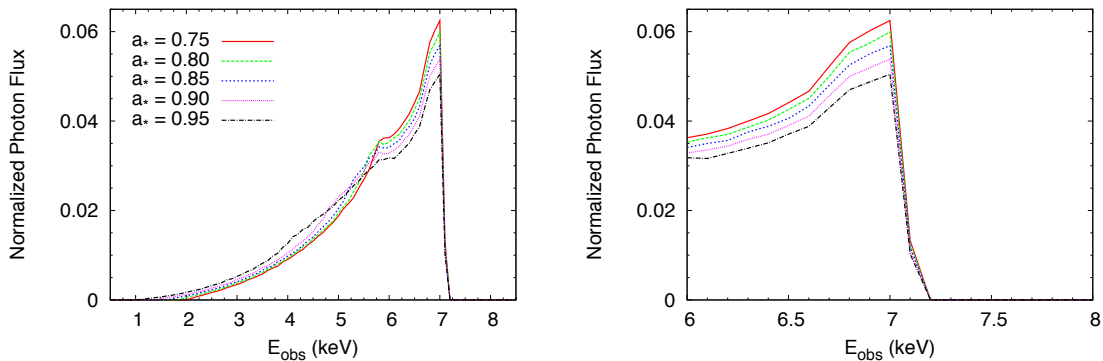


Figure 3. Iron line profile for different values of the spin parameter a_* (the right panel is just the enlargement of the left one in the energy range 6-8 keV). The other parameters are: viewing angle $i = 45^\circ$, inner radius $r_{\text{in}} = r_{\text{ISCO}}$, outer radius $r_{\text{out}} = r_{\text{ISCO}} + 100 r_g$, index of emissivity profile $q = 3$.

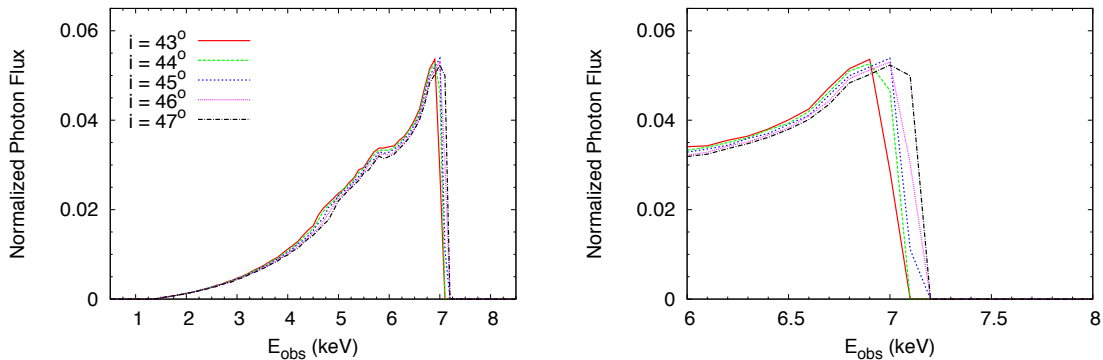


Figure 4. Iron line profile for different values of the viewing angle i (the right panel is just the enlargement of the left one in the energy range 6-8 keV). The other parameters are: spin parameter $a_* = 0.9$, inner radius $r_{\text{in}} = r_{\text{ISCO}}$, outer radius $r_{\text{out}} = r_{\text{ISCO}} + 100 r_g$, index of emissivity profile $q = 3$.

from the one of the other parameters. Such a statement can be quantitatively justified with the error analysis described below. For a crude estimate aiming at showing the basic idea of the proposal of the present paper, we can restrict the attention only to the viewing angle when we constrain possible variations of the fine structure constant.

The value of the $K\alpha$ iron line in the strong gravitational field of a black hole can be estimated by comparing the iron line profile with $E = 6.4$ keV and the angle inferred by the iron line fit (column 5 in Table I) with the profiles calculated with the “actual” energy E (which may be different from 6.4 keV because of a different value of α) and the angle obtained from dynamical/jet measurements (column 2 in Table I). The latter are clearly independent of the values of fundamental constants close to the compact object. If the other parameter

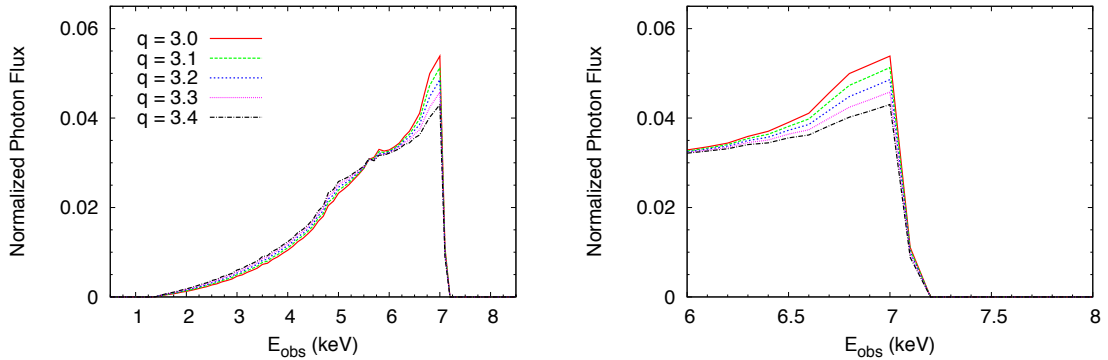


Figure 5. Iron line profile for different values of the index of emissivity profile q (the right panel is just the enlargement of the left one in the energy range 6-8 keV). The other parameters are: spin parameter $a_* = 0.9$, viewing angle $i = 45^\circ$, inner radius $r_{\text{in}} = r_{\text{ISCO}}$, outer radius $r_{\text{out}} = r_{\text{ISCO}} + 100 r_g$.

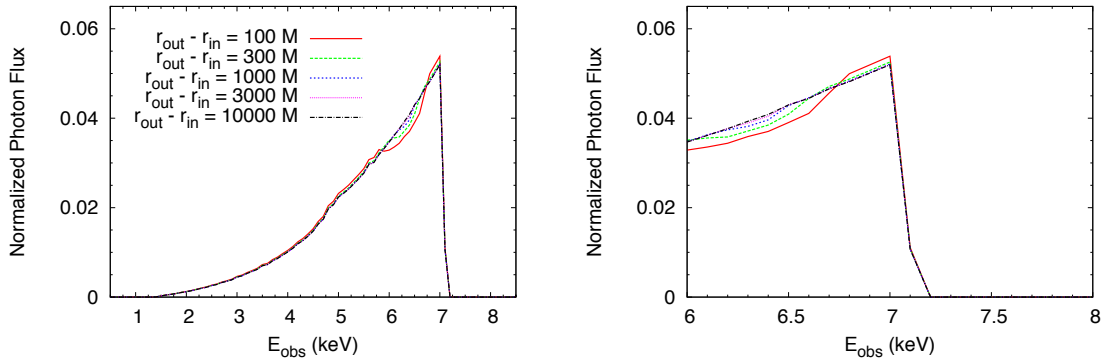


Figure 6. Iron line profile for different values of the outer radius r_{out} (the right panel is just the enlargement of the left one in the energy range 6-8 keV). The other parameters are: spin parameter $a_* = 0.9$, viewing angle $i = 45^\circ$, inner radius $r_{\text{in}} = r_{\text{ISCO}}$, index of emissivity profile $q = 3$.

are fixed, the reduced χ^2 is

$$\begin{aligned} \chi_{\text{red}}^2(E_{K\alpha}) &= \frac{\chi^2}{n-p} = \\ &= \frac{1}{n-p} \sum_{i=1}^n \frac{\left[N_i(E_{K\alpha}, \tilde{a}_*, \tilde{i}, \tilde{q}, \tilde{r}_{\text{out}}) - N_i(\tilde{E}_{K\alpha}, \tilde{a}_*, \tilde{i}_{\text{iron}}, \tilde{q}, \tilde{r}_{\text{out}}) \right]^2}{\sigma_i^2}, \quad (\text{C.1}) \end{aligned}$$

where the summation is performed over n sampling energies E_i , p is the number of free parameters in the model being fitted (here $p = 1$), and N_i is the normalized photon fluxes in the energy bin $[E_i, E_i + \Delta E]$. \tilde{a}_* , \tilde{i}_{iron} , \tilde{q} , and \tilde{r}_{out} have the values measured by the iron line fit, while \tilde{i} has the one inferred by the optical/near-infrared light curve observations or jet measurements. $\tilde{E}_{K\alpha} = 6.4$ keV. The resulting energy $E_{K\alpha}$ is the one that minimizes the reduced χ^2 . This provides the central value of $\Delta\alpha/\alpha$ in the last column of Table I in the paper. The ΔE used in these calculations is 100 keV, which is roughly the resolution of

current X-ray facilities, and the summation is performed over a small energy range of 2 keV around the peak of the line. While data are often more sensitive to lower energies, depending on the detector and its effective area, because of the reduced energy range here the same weighting has been assigned to different energies.

The uncertainty on $\Delta\alpha/\alpha$ reported in Tab. I is obtained by replacing the $1\text{-}\sigma$ values of \tilde{i} and \tilde{i}_{iron} in Eq. (C.1). If we compute

$$\chi_{\text{red}}^2(E_{K\alpha}) = \frac{1}{n-p} \sum_{i=1}^n \frac{\left[N_i(E_{K\alpha}, \tilde{a}_*, \tilde{i} \pm \Delta\tilde{i}, \tilde{q}, \tilde{r}_{\text{out}}) - N_i(\tilde{E}_{K\alpha}, \tilde{a}_*, \tilde{i}_{\text{iron}} \pm \Delta\tilde{i}_{\text{iron}}, \tilde{q}, \tilde{r}_{\text{out}}) \right]^2}{\sigma_i^2}, \quad (\text{C.2})$$

we get four different energies (coming from the four different combinations of $\tilde{i} \pm \Delta\tilde{i}$ and $\tilde{i}_{\text{iron}} \pm \Delta\tilde{i}_{\text{iron}}$). We can then take the two extreme values as upper and lower values of $\Delta\alpha/\alpha$. As we are considering only the central value for the other model parameters (\tilde{a}_* , \tilde{q} , and \tilde{r}_{out}), neglecting their uncertainty, it is not really important the energy range under consideration, in the sense that the final result does not depend on this choice.

For instance, if we consider the values reported in Ref. [36] for the black hole in Cygnus X-1, this approach gives $E = 6.46$ keV as central value of the energy, while the lower and upper bounds are, respectively, $E = 6.42$ keV (when $i = 27.9^\circ$ and $i_{\text{iron}} = 29^\circ$) and $E = 6.49$ keV (when $i = 26.3^\circ$ and $i_{\text{iron}} = 31^\circ$). So, $\Delta\alpha/\alpha = +0.005 \pm 0.003$. The results in Ref. [37] give $E = 6.50$ keV as central value, and $E = 6.44$ keV (when $i = 27.9^\circ$ and $i_{\text{iron}} = 30^\circ$) and $E = 6.56$ keV (when $i = 26.3^\circ$ and $i_{\text{iron}} = 34^\circ$) as, respectively, lower and upper ones. The constraint on the fine structure constant is $\Delta\alpha/\alpha = +0.008 \pm 0.005$.

If we want to include the uncertainty of the other parameters, we can proceed as follows. For instance, including the effect of the uncertainty of the spin we can write

$$\chi_{\text{red}}^2(E_{K\alpha}) = \frac{1}{n-p} \sum_{i=1}^n \frac{1}{\sigma_i^2} \left[N_i(E_{K\alpha}, \tilde{a}_* \pm \Delta\tilde{a}_*, \tilde{i} \pm \Delta\tilde{i}, \tilde{q}, \tilde{r}_{\text{out}}) + N_i(\tilde{E}_{K\alpha}, \tilde{a}_* \pm \Delta\tilde{a}_*, \tilde{i}_{\text{iron}} \pm \Delta\tilde{i}_{\text{iron}}, \tilde{q}, \tilde{r}_{\text{out}}) \right]^2, \quad (\text{C.3})$$

and find the minimum of the reduced χ^2 . If we restrict the analysis to the very small energy range including the peak and higher energies, we see that the effect of the uncertainty on a_* is roughly an order of magnitude smaller. The uncertainty on q and \tilde{r}_{out} also produces small effects. A proper error search over multiple parameters could be done better with multivariate gaussian draws from the parameter distribution.

Acknowledgments

I thank Antonino Marciano, James Steiner, and Naoki Tsukamoto for useful comments and suggestions. This work was supported by the NSFC grant No. 11305038, the Shanghai Municipal Education Commission grant for Innovative Programs No. 14ZZ001, the Thousand Young Talents Program, and Fudan University.

References

- [1] C. M. Will, Living Rev. Rel. **9**, 3 (2006) [gr-qc/0510072].

- [2] P. Jordan, *Naturwiss.* **25**, 513 (1937).
- [3] C. Brans and R. H. Dicke, *Phys. Rev.* **124**, 925 (1961).
- [4] W. J. Marciano, *Phys. Rev. Lett.* **52**, 489 (1984).
- [5] Y. -S. Wu and Z. Wang, *Phys. Rev. Lett.* **57**, 1978 (1986).
- [6] K. -i. Maeda, *Mod. Phys. Lett. A* **3**, 243 (1988).
- [7] T. R. Taylor and G. Veneziano, *Phys. Lett. B* **213**, 450 (1988).
- [8] T. Damour and A. M. Polyakov, *Nucl. Phys. B* **423**, 532 (1994) [hep-th/9401069].
- [9] T. Damour, F. Piazza and G. Veneziano, *Phys. Rev. Lett.* **89**, 081601 (2002) [gr-qc/0204094].
- [10] T. Damour, F. Piazza and G. Veneziano, *Phys. Rev. D* **66**, 046007 (2002) [hep-th/0205111].
- [11] J. -P. Uzan, *Rev. Mod. Phys.* **75**, 403 (2003) [hep-ph/0205340].
- [12] J. -P. Uzan, *Living Rev. Rel.* **14**, 2 (2011) [arXiv:1009.5514 [astro-ph.CO]].
- [13] T. Rosenband *et al.*, *Science* **319**, no. 5871, 1808 (2008).
- [14] J. K. Webb, V. V. Flambaum, C. W. Churchill, M. J. Drinkwater and J. D. Barrow, *Phys. Rev. Lett.* **82**, 884 (1999) [astro-ph/9803165].
- [15] J. K. Webb *et al.*, *Phys. Rev. Lett.* **87**, 091301 (2001) [astro-ph/0012539].
- [16] J. K. Webb *et al.*, *Phys. Rev. Lett.* **107**, 191101 (2011) [arXiv:1008.3907 [astro-ph.CO]].
- [17] J. C. Berengut *et al.*, *Phys. Rev. Lett.* **111**, 010801 (2013) [arXiv:1305.1337 [astro-ph.CO]].
- [18] A. C. Fabian, M. J. Rees, L. Stella and N. E. White, *Mon. Not. Roy. Astron. Soc.* **238**, 729 (1989).
- [19] P. Barr, N. E. White and C. G. Page, *Mon. Not. Roy. Astron. Soc.* **216**, 65 (1985).
- [20] A. C. Fabian, K. Iwasawa, C. S. Reynolds and A. J. Young, *Publ. Astron. Soc. Pac.* **112**, 1145 (2000) [astro-ph/0004366].
- [21] C. S. Reynolds and M. A. Nowak, *Phys. Rept.* **377**, 389 (2003) [astro-ph/0212065].
- [22] T. Dauser, J. Garcia, J. Wilms, M. Bock, L. W. Brenneman, M. Falanga, K. Fukumura and C. S. Reynolds, *Mon. Not. Roy. Astron. Soc.* **430**, 1694 (2013) [arXiv:1301.4922 [astro-ph.HE]].
- [23] A. C. Fabian *et al.*, *Mon. Not. Roy. Astron. Soc.* **424**, 217 (2012) [arXiv:1204.5854 [astro-ph.HE]].
- [24] Y. Lu and D. F. Torres, *Int. J. Mod. Phys. D* **12**, 63 (2003) [astro-ph/0205418].
- [25] C. Bambi, *Phys. Rev. D* **87**, 023007 (2013) [arXiv:1211.2513 [gr-qc]].
- [26] C. Bambi, *Phys. Rev. D* **87**, 084039 (2013) [arXiv:1303.0624 [gr-qc]].
- [27] C. Bambi, *JCAP* **1308**, 055 (2013) [arXiv:1305.5409 [gr-qc]].
- [28] C. Bambi and D. Malafarina, *Phys. Rev. D* **88**, 064022 (2013) [arXiv:1307.2106 [gr-qc]].
- [29] J. M. Bardeen and J. A. Petterson, *Astrophys. J.* **195**, L65 (1975).
- [30] T. J. Maccarone, *Mon. Not. Roy. Astron. Soc.* **336**, 1371 (2002) [astro-ph/0209105].
- [31] J. F. Steiner and J. E. McClintock, *Astrophys. J.* **745**, 136 (2012) [arXiv:1110.6849 [astro-ph.HE]].
- [32] J. A. Orosz *et al.*, *Astrophys. J.* **742**, 84 (2011) [arXiv:1106.3689 [astro-ph.HE]].
- [33] R. P. Fender *et al.*, *Mon. Not. Roy. Astron. Soc.* **304**, 865 (1999) [astro-ph/9812150].
- [34] R. Shafee *et al.*, *Astrophys. J.* **636**, L113 (2006) [astro-ph/0508302].

- [35] J. A. Orosz *et al.*, *Astrophys. J.* **730**, 75 (2011) [arXiv:1101.2499 [astro-ph.SR]].
- [36] J. M. Miller, C. S. Reynolds, A. C. Fabian, G. Miniutti and L. C. Gallo, *Astrophys. J.* **697**, 900 (2009) [arXiv:0902.2840 [astro-ph.HE]].
- [37] R. Duro *et al.*, *Astron. Astrophys.* **533**, L3 (2011) [arXiv:1108.1157 [astro-ph.HE]].
- [38] J. A. Tomsick *et al.*, *Astrophys. J.* **780**, 78 (2014) [arXiv:1310.3830 [astro-ph.HE]].
- [39] J. M. Miller *et al.*, *Astrophys. J.* **775**, L45 (2013) [arXiv:1308.4669 [astro-ph.HE]].
- [40] J. F. Steiner *et al.*, *Mon. Not. Roy. Astron. Soc.* **416**, 941 (2011) [arXiv:1010.1013 [astro-ph.HE]].
- [41] L. Gou *et al.*, *Astrophys. J.* **742**, 85 (2011) [arXiv:1106.3690 [astro-ph.HE]].
- [42] J. F. Steiner, private communications.
- [43] L. M. Krauss and F. Wilczek, *Phys. Rev. Lett.* **62**, 1221 (1989).
- [44] P. Bizon, *Phys. Rev. Lett.* **64**, 2844 (1990).
- [45] M. S. Volkov and D. V. Galtsov, *Sov. J. Nucl. Phys.* **51**, 747 (1990).
- [46] B. Kleihaus, J. Kunz and E. Radu, *Phys. Rev. Lett.* **106**, 151104 (2011) [arXiv:1101.2868 [gr-qc]].
- [47] G. Dvali and C. Gomez, *Phys. Lett. B* **719**, 419 (2013) [arXiv:1203.6575 [hep-th]].
- [48] C. W. Misner, K. S. Thorne and J. A. Wheeler, *Gravitation* (W. H. Freeman, San Francisco, US, 1973)